Effect of Seawater Chlorination on the Erosion Corrosion Behaviour of CuNi90/10

W. Schleich[1], R. Feser[2], G. Schmitt[2], S. Haarmann[2], K. Schnier[2]

[1]KME Germany AG
Klosterstr. 29, D-49023 Osnabrück, Germany
wilhelm.schleich@kme.com

[2] Laboratory for Corrosion Protection
Iserlohn University of Applied Sciences
Frauenstuhlweg 31; D-58644 Iserlohn; Germany
feser.r@fh-swf.de; schmitt.g@fh-swf.de

Abstract

The influence of dissolved sodium hypochlorite on the flow resistance of UNS C70600 (CuNi90/10) in artificial ASTM seawater at room temperature was investigated electrochemically with the rotatimg disc and gravimetrically with the rotating cage experiments. The performance of the material is improved by protective film formation during 6 weeks pre-exposure in hypochlorite-free artificial seawater at room temperature. For a pre-exposed surface state, up to 5 ppm hypochlorite is acceptable without significantly impairing the flow resistance and the general corrosion rate. The critical wall shear stress for all media tested is above 200 Pa indicating that the flow resistance is significantly higher than expected from data in the literature (43 Pa).

Keywords: UNS C70600, CuNi90/10, seawater, chlorination, flow intensities, wall shear stress, erosion corrosion, flow induced localized corrosion, rotating disc, rotating cage

1 Introduction

The impact of seawater on materials performance is determined by numerous parameters such as condition of the material, system design, fabrication procedure, seawater temperature, flow intensity, biological activity, and presence of oxidizing compounds. Over several decades, many thousands of tons of copper-nickel alloys have been installed in different marine engineering structures used in the

shipbuilding, offshore, power and desalination industries. The workhorse is the alloy UNS C70600 (CuNi90/10, cupronickel, CuNi10Fe1Mn) which exhibits widespread applicability. With its iron content of 1.5 to 2.0 w.% (Table 1) this alloy provides optimum resistance to flowing seawater (Fig. 1).

***Table 1**: Comparison of chemical composition between various specifications for cupronickel 90/10 used as tubing material*

Standard	DIN/EN	ASTM	ISO	EEMUA	KME
Designation	CuNi10Fe1Mn		CuNi10Fe1Mn		CuNi10 Fe1,6Mn
Ref. No.	2.0872/CW352H	UNS C70600		UNS 7060X	
Copper	Rem.	Rem.	Rem.	Rem.	Rem.
Nickel	9.0-11.0	9.0-11.0	9.0-11.0	10.0-11.0	10.0-11.0
Iron	1.0-2.0	1.0-1.8	1.0-2.0	1.5-2.00	1.50-1.8
Manganese	0.5-1.0	1.0	0.5-1.0	0.5-1.0	0.6-1.0
Tin	0.03	-	0.03	-	0.03
Carbon	0.05	0.05	0.05	0.05	0.02
Lead	0.02	0.02	0.02	0.01	0.01
Phosphorus	0.02	0.2	0.02	0.02	0.02
Sulphur	0.05	0.02	0.02	0.02	0.005
Zinc	0.05	0.5	0.5	0.2	0.05
Cobalt	0.1	-	0.05	-	0.1
Impurities	0.2	-	0.1	0.3	0.02

Single values represent the maximum content.

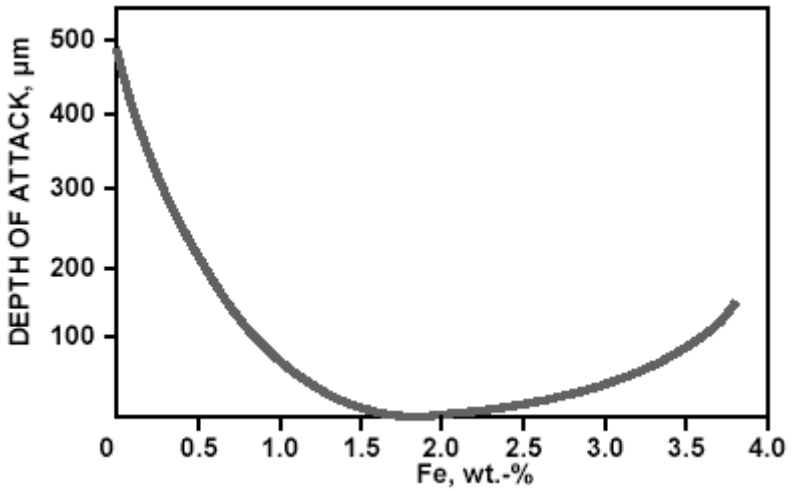

***Figure 1:**. Influence of iron content on depth of impingement attack on UNS C70600 in seawater after 30 days exposure at 3 m/s.[1]*

Neither general corrosion nor pitting corrosion is a problem for CuNi90/10 in natural clean seawater or in seawater chlorinated to levels sufficient to control biological activity. However, localized corrosion may occur in polluted and stagnant seawater under conditions of deposit formation and in the presence of sulfide [2-4] mostly originating from the activity of sulfate reducing bacteria. Another reason for localized attack could be erosion corrosion initiated by flowing seawater. However, flow induced localized corrosion (FILC) is likely to occur only above critical local flow intensities creating local energy densities which are high enough to break down protective scales, layers or films on the metal surface [5-7]. Critical flow intensities are often given in terms of critical flow velocities. However, it has to be kept in mind that such data are not independent of geometry, e.g. the inner diameter when considering piping. Critical flow velocities in UNS C70600 piping for seawater at 27°C were estimated to be 4.4 m/s for a tube with 0.03 m in diameter and 6.0 m/s for a tube with 3 m in diameter [8]. The industrially accepted critical flow velocity in large piping for unpolluted seawater has been conservatively set in the range between 3.5 and to 3.6 $m \cdot s^{-1}$ [8-11].

A more general description of flow intensities is possible in terms of wall shear stresses which relate more closely to the interaction between the flowing fluid and the wall. Therefore, maximum design velocities in UNS C70600 piping for seawater have been related to pipe diameters based on measurements of critical wall shear stresses (Fig. 2) [8]. The critical wall shear stress for the initiation of FILC in this material has been calculated to amount to 43 Pa (N/m^2) [8]. Critical flow parameters for UNS C70600 tubing are collected in Table 2. The critical flow velocities given here appear to be rather conservative. Experimental results are available which indicate that much higher flow velocities, e.g. in the range of 10 to 15 m/s, may be acceptable, specifically for emergency situations, as in fire fighting systems [12]. Even with sand loaded seawater velocities of 7 m/s in 4" to 7" pipes yielded no appreciable corrosion attack [13].

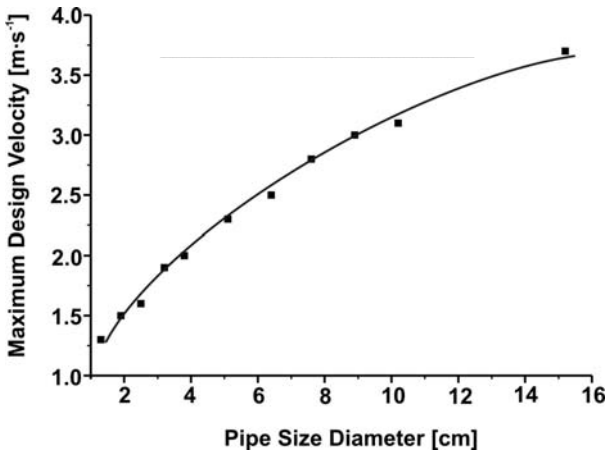

Figure 2: *Maximum design velocities of CuNi90/10 piping for seawater [8]*

Table 2: *Critical flow parameters for CuNi90/10 tubing in seawater [8-10]*

Critical Shear Stress [$N \cdot m^{-2}$]	43
Crit. Velocity in 25 mm Tube [$m \cdot s^{-1}$]	4.3
Maximum Tubular Design Velocity [$m \cdot s^{-1}$] (based on 50% critical shear stress)	2.9
Maximum Tubular Design Velocity [$m \cdot s^{-1}$]	3.0 - 3.6

The data given above relate to non-chlorinated seawater. It is not clear whether the presence of chlorine-containing additives will change the flow resistance of UNS C70600 in seawater within relevant concentration ranges. Basically it is industrially accepted that chlorine concentrations of 0.2 to 0.5 ppm exert no negative effects [4] (normally 0.25 ppm chlorine is sufficient to 100% control microbiological activity [2]). For continuous and intermittent chlorine additions, concentrations of 0.3 and 0.5 ppm, respectively, are recommended [14, 15]. All previous investigators agree on the threshold values given above and that over-chlorination should be avoided. However, they also recommend more additional research specifically on the effect of over-chlorination which presently is not sufficiently understood and experimentally backed-up.

In the first part of this project it was demonstrated [16] that the influence of chlorine on the corrosion rate under stagnant conditions is not strong and the quality of the oxide layer is not affected by the presence of chlorine. It was the aim of the present work to study the effect of chlorine-containing additive at higher concentrations on critical flow intensies to initiate FILC at UNS C70600 in artificial seawater (ASTM 1441). The material's surface was tested both in the as-delivered and in the pre-exposed condition. Pre-exposure for 6 weeks at room temperature in stagnant ASTM seawater produces corrosion product films known to be protective [17].

2 Experimental

The corrosion system was defined to consist of standard quality CuNi90/10 soft annealed material with as-delivered and pre-exposed surfaces, artificial seawater according to ASTM 1441 with a pH of 8.2 and sodium hypochlorite as oxidizing agent in the concentrations 0, 0.3, 0.5, 1.0, 3.0 and 5.0 ppm. All experiments were performed at ambient (room) temperature with access of air to the corrosion medium.

The influence of hypochlorite additions on the electrochemical behaviour of the material tested under flow conditions was investigated with the rotating disc. The critical flow intensities for initiation of FILC were evaluated with the rotating cage.

2.1 Rotating Disc Experiments

Disc samples with a diameter of 10 mm were machined from CuNi90/10 rods and fixed in a PTFE-holder (Fig. 3) which was mounted on the shaft of a stirrer. Prior to experiments with an as-delivered material surface, the disc surface was ground with emery paper progressing from coarse to finer grain size (1000, 2500, 4000) and finally polished. After degreasing with acetone and subsequent drying with oil-free compressed air, the electrochemical experiment was started. For experiments with pre-exposed material surface, the disc samples which were already fixed in the

PTFE-holder and had been ground, polished and degreased, were exposed for 6 weeks in hypochlorite-free artificial seawater (ASTM 1441) at room temperature with access to air. The disc holder was then mounted on the shaft without further surface treatment.

The prepared disc electrode was positioned in a 1.5 ltr. double-walled beaker filled with 1.3 ltr. of test liquid which was taken from a 10 ltr. stock solution. The concentration of sodium hypochlorite added to the test solution was controlled with a colorimetric analysis using the „CHECKIT Comperator“ purchased from Tintometer Company. The potentiodynamic polarisation measurements were performed with a saturated Ag/AgCl reference electrode and a platinum net as counter electrode. In all polarisation runs the disc working electrode was rotated with a rotation speed of 1000 rpm. Prior to the polarisation measurements which were performed with a potential scan rate of 0.06 mV/s the rest potential was measured for at least 10 minutes.

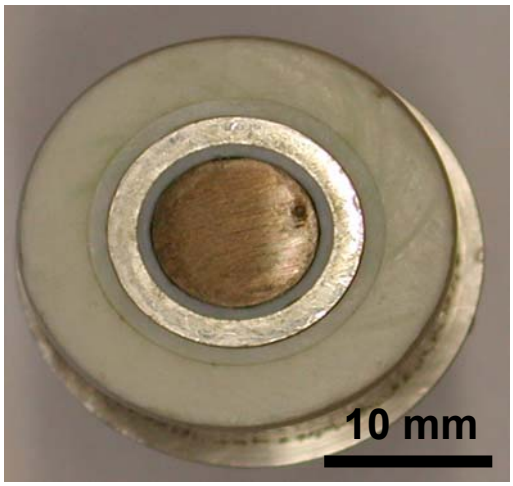

Fig. 3: *Rotating disc*

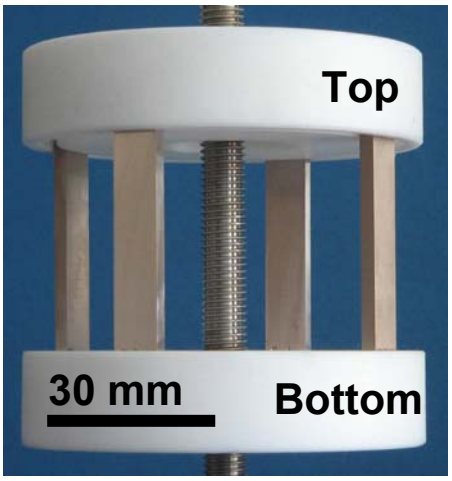

Fig. 4: *Rotating cage*

2.2 Rotating Cage Experiments

The rotating cage (Fig. 4) is frequently used to screen the susceptibility of materials to FILC [18-20]. Due to the many experimental advantages and the successful use of rotating cage data in service, attempts have been made to quantify the flow intensities encountered at coupons rotated in the rotating cage. Equ. 1 was developed as an approximation to estimate the maximum wall shear stress at coupons in the rotated cage [19, 20]:

$$\tau_{RC} = 0.0791 \cdot \mathrm{Re}_{RC}^{-0.3} \cdot \rho \cdot r_{RC}^{2} \cdot \omega^{2.3} \qquad (1)$$

where τ_{RC} is the wall shear stress in rotated cage [Pa], Re_{RC} is the Reynolds number of rotating cage ($\mathrm{Re}_{RC} = \frac{\omega \cdot r_{RC}^{2}}{\nu}$), r_{RC} is the radius of the rotating cage [m], ρ is the solution density [kg·m^{-3}], ω is the rotational speed [s^{-1}] .

This equation is valid only for a certain geometry of the rotated cage with a certain number of coupons in a certain position without applying baffles to prevent rotation of

the liquid by drag through the rotated cage. Comparison of critical wall shear stresses obtained from both rotating cage and jet impingement [21,22] experiments for the same corrosion system revealed that the critical wall shear stresses calculated according to Equ. 1 are at least a factor of 2 higher than the values received via Equ. 2 for the impinging jet [21, 22].

$$\tau_w = 0.0447 \cdot \rho \cdot u_0^2 \cdot \mathrm{Re}^{-0.182} \left(\frac{x}{d}\right)^{-2} \qquad (2)$$

where u is the flow velocity [m·s^{-1}], d the diameter of the jet nozzle and x the distance from the center of the jet on the impinged surface.

In a separate investigation within a joint industry project (JIP) another set of equations has been experimentally developed for the quantification of local wall shear stresses at characteristic sites of coupon surfaces (Fig. 5) rotated in the cage [23, 24]. The highest wall shear stresses were found at the inner edge in the middle of the leading edge of a rotated coupon. At this site the mean wall shear stress can be calculated according to Equ. 3, and the 95th percentile of the instantaneous wall shear stress according to Equ. 4. The constants a, b and c in Equs. 3 and 4 will be reported in a future publication.

$$\tau_{mean} = a \cdot RPM^b \cdot \eta^c \qquad (3)$$

$$\tau_{95} = 1.78 \cdot a \cdot RPM^b \cdot \eta^c \qquad (4)$$

(*RPM* = rounds per minute)

It appeared that critical wall shear stresses evaluated via Equ. 4 match reasonably well with the critical wall shear stresses obtained via Equ. 2 in jet impingment experiments. No acceptable match could be reached using Equ. 1. This problem will be discussed in a future publication.

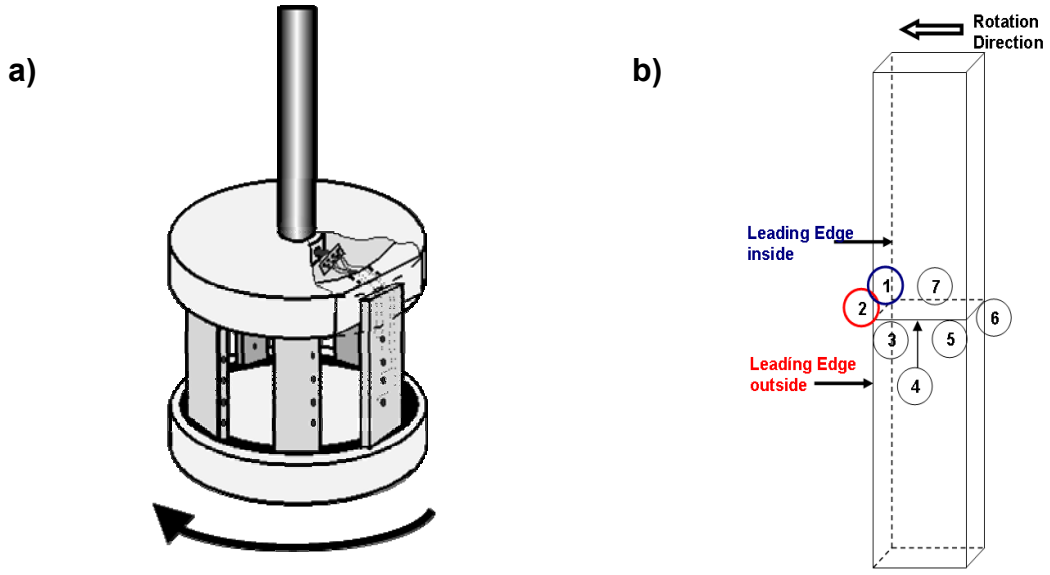

Fig. 5: *Microelectrochemical measurement of local wall shear stresses at characteristic surface sites on coupons rotated in the cage [23, 24]*

For the geometric conditions used in the rotating cage experiments during the present study the calculated maximum wall shear stress at the inner corner in the middle of the leading edge of the rotated coupon (position 1 in Fig. 5) amounted to 200 Pa at a rotation speed of 1500 rpm.

The experimental setup in the rotating cage experiments is shown in Fig. 6. The rotating cage according to Fig. 4 was filled equidistantly with 4 UNS C70600 coupons (50x10x3mm). Two of the coupons were in the as-received surface state (machined surface, finely ground, polished and degreased with aceton), while the other two coupons were in the pre-exposed surface state. Pre-exposure occured by exposing the coupons at room temperature for 6 weeks in hypochlorite-free artificial ASTM seawater under access of air. The coupons had been weighed before mounting in the rotated cage and before pre-exposure in seawater, respectively.

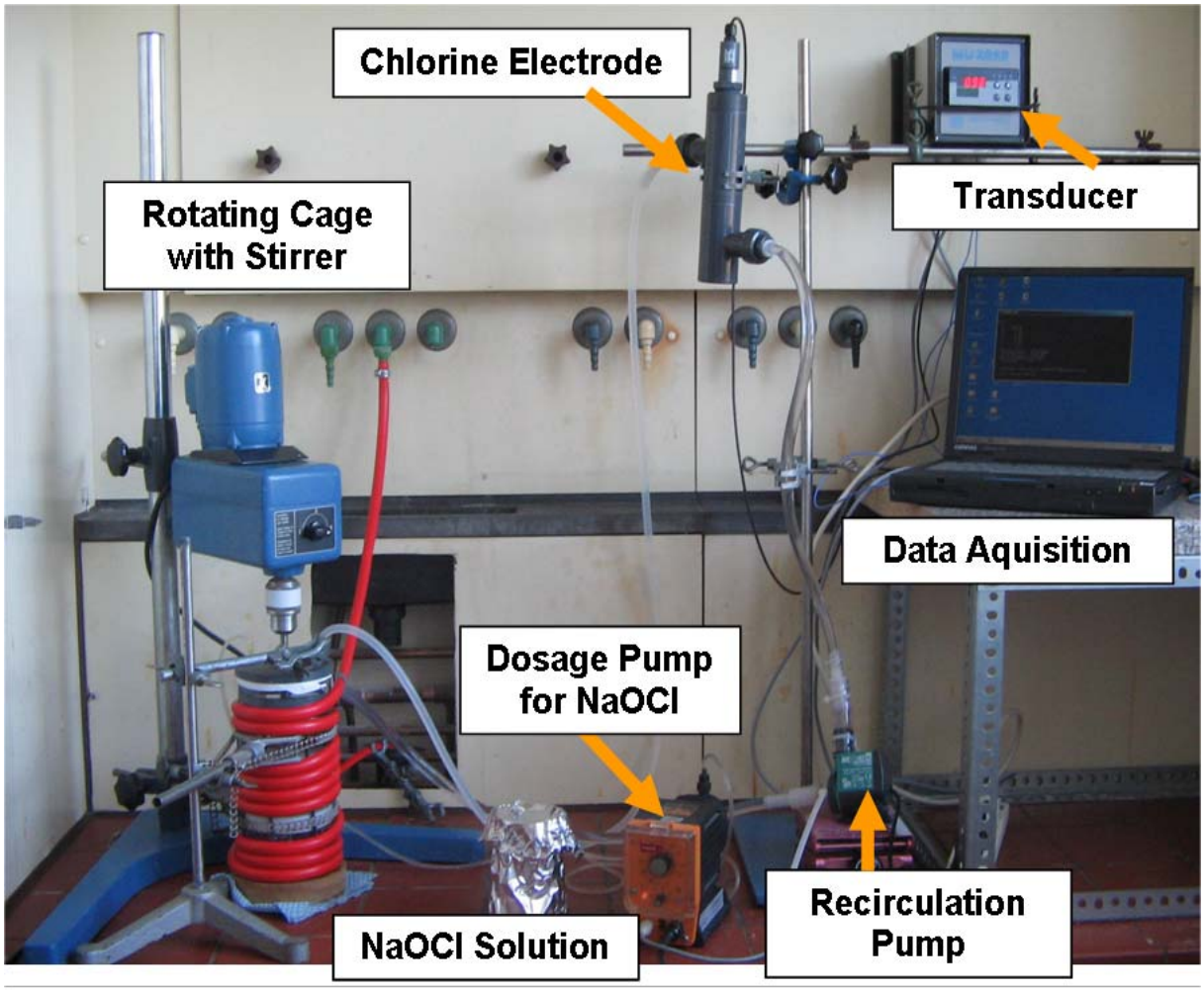

Figure 6: *Experimental setup for rotating cage experiments in NaOCl-containing artificial seawater*

The cage was positioned in a water-thermostated glass cylinder filled with 1.6 ltr. of test liquid and closed with a splash lid. During the 96 h test time the cage was rotated with rotation speeds between 850 and 1500 rpm, and the test liquid was recirculated at room temperature via a recirculation pump over a chlorine/ hypochlorite electrode (model CS2.3, Sensortechnik Meinsberg GmbH, Germany), which measured the hypochlorite concentration and - via a transducer (MU2060, Sensortechnik Meinsberg GmbH) - triggered a NaOCl dosage pump which metered NaOCl solution into the test liquid to keep the hypochlorite concentration constant at 1 or 5 ppm (Fig. 7). Indicated via a digital display the amperometric measurement yielded the concentration of “free chlorine” (including chlorine + hypochlorite) with an accuracy of

0.01 mg/L. The measuring interval was 2 minutes. The electrode was calibrated with the „CHECKIT Comperator“ (Tintometer Company) using a colorimetric method. The pH of the liquid was kept constant at pH 8.2. As can be seen from the diagramme in Fig. 8, the chlorine concentration at pH 8.2 is close to zero and the prevailing oxidizing compound is the hypochlorite anion and the hypochloric acid.

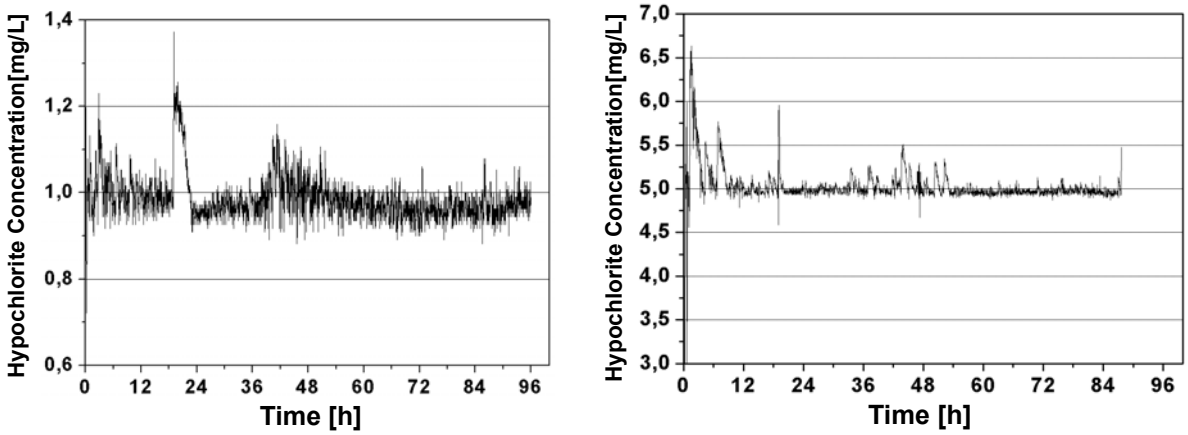

***Figure 7**: Recordings of hypochlorite concentration in the test liquid (examples for runs with 1 ppm and 5 ppm hypochlorite)*

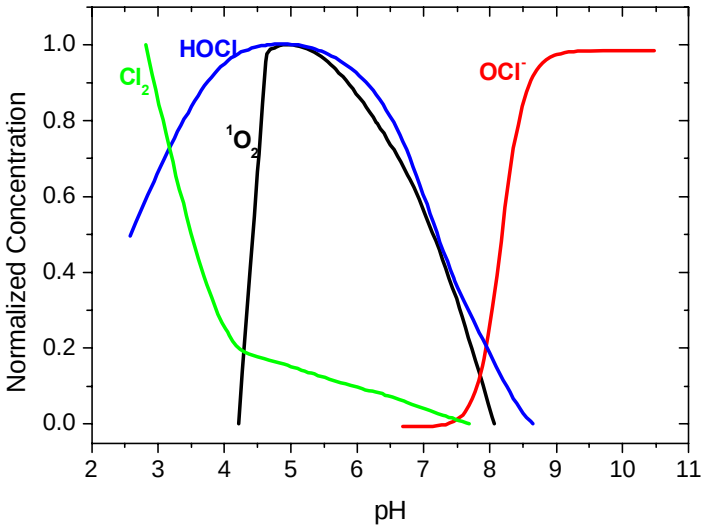

***Fig. 8:** Effect of pH on the chlorine concentration in hypochlorite-containing waters [25]*

3 Results and Discussion

3.1 Electrochemicial Measurements with the Rotating Disc

Polarisation measurements at 1000 rpm with as-delivered and seawater pre-exposed electrode surfaces revealed that the rest potential expectedly shifts in both cases to more positive values when the hypochlorite concentration is stepwise increased from zero to 5 ppm (Fig. 9). However, the rest potentials at as-delivered surfaces (Fig. 9a) were found to be significantly more negative than the corresponding rest potentials

measured at the scaled surface resulting from 6 weeks pre-exposure in the artificial salt water (Fig. 9b).

With increasing hypochlorite concentration a steady increase in the corrosion current densities was observed for the as-delivered, unscaled surface. This effect was much less pronounced in polarisation measurements with pre-exposed, scaled surfaces. Up to a hypochlorite concentration of 0.5 ppm no significant increase in the corrosion current densities was found, although the rest potential shifted considerably to more positive values.The protecting effect of the scale formed during pre-exposure diminished at hypochlorite concentrations above 1 ppm (Fig. 9b).

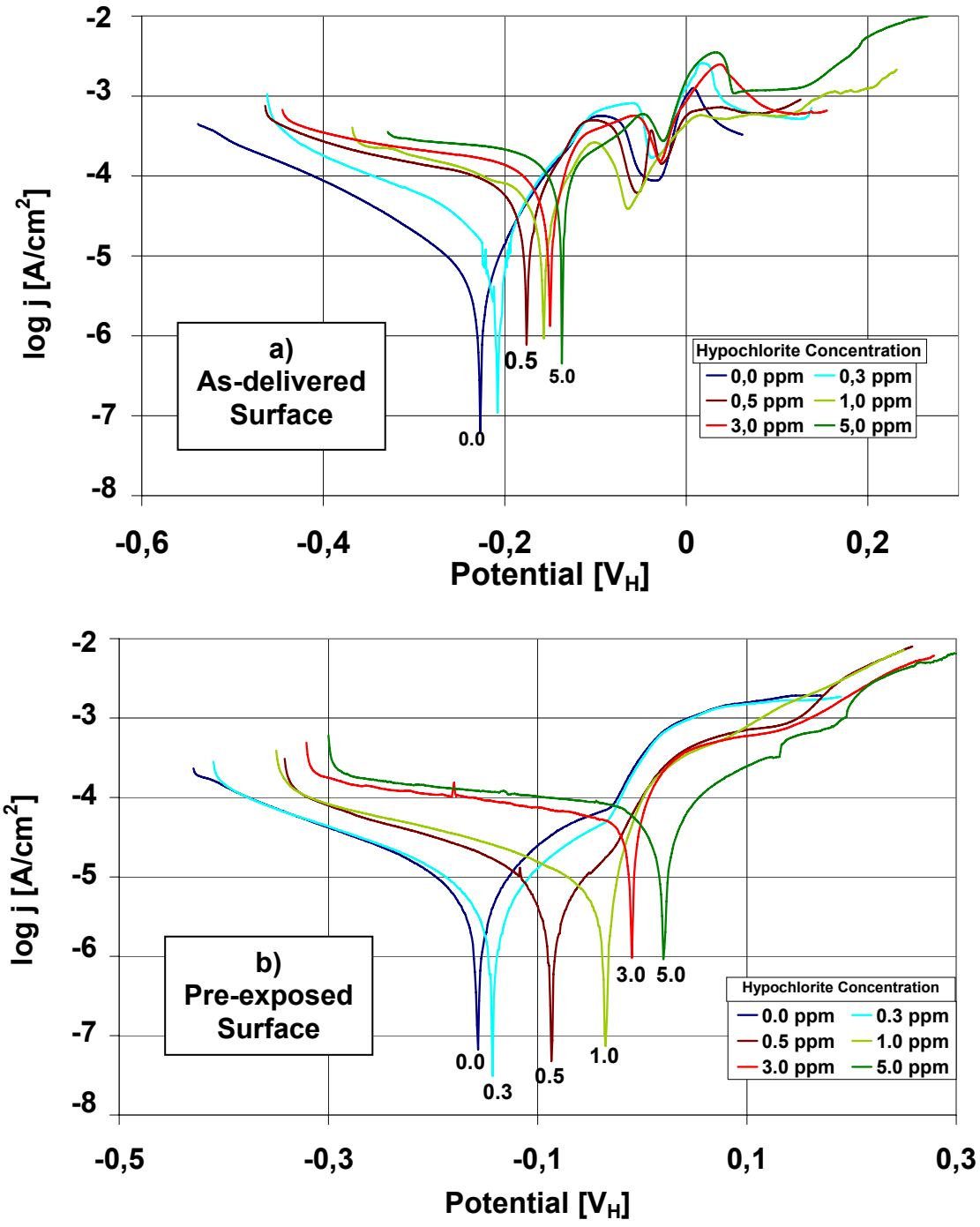

***Figure 9**: Current density-potential curves of CuNi90/10 with as-delivered (a) and seawater pre-exposed (b) surface in artificial ASTM seawater at pH 8.2 with different concentrations of NaOCl*

3.2 Experiments with the Rotating Cage

Rotating cage experiments were performed to determine whether the beneficial scale effect contributes also to the level of critical wall shear stresses. Runs with rotation speeds of 850 and 1000 rpm yielded no FILC within 4 days exposure in artificial seawater regardless of the presence of hypochlorite with concentrations up to 5 ppm. It needed a rotation speed of 1500 rpm to start FILC at least slightly at the leading edges of the coupons, i.e. at the sites of maximum flow intensity. This result was obtained in the absence as well as in the presence of hypochlorite up to concentrations of 5 ppm, regardless of the nature of coupon surface (as-received or pre-exposed).

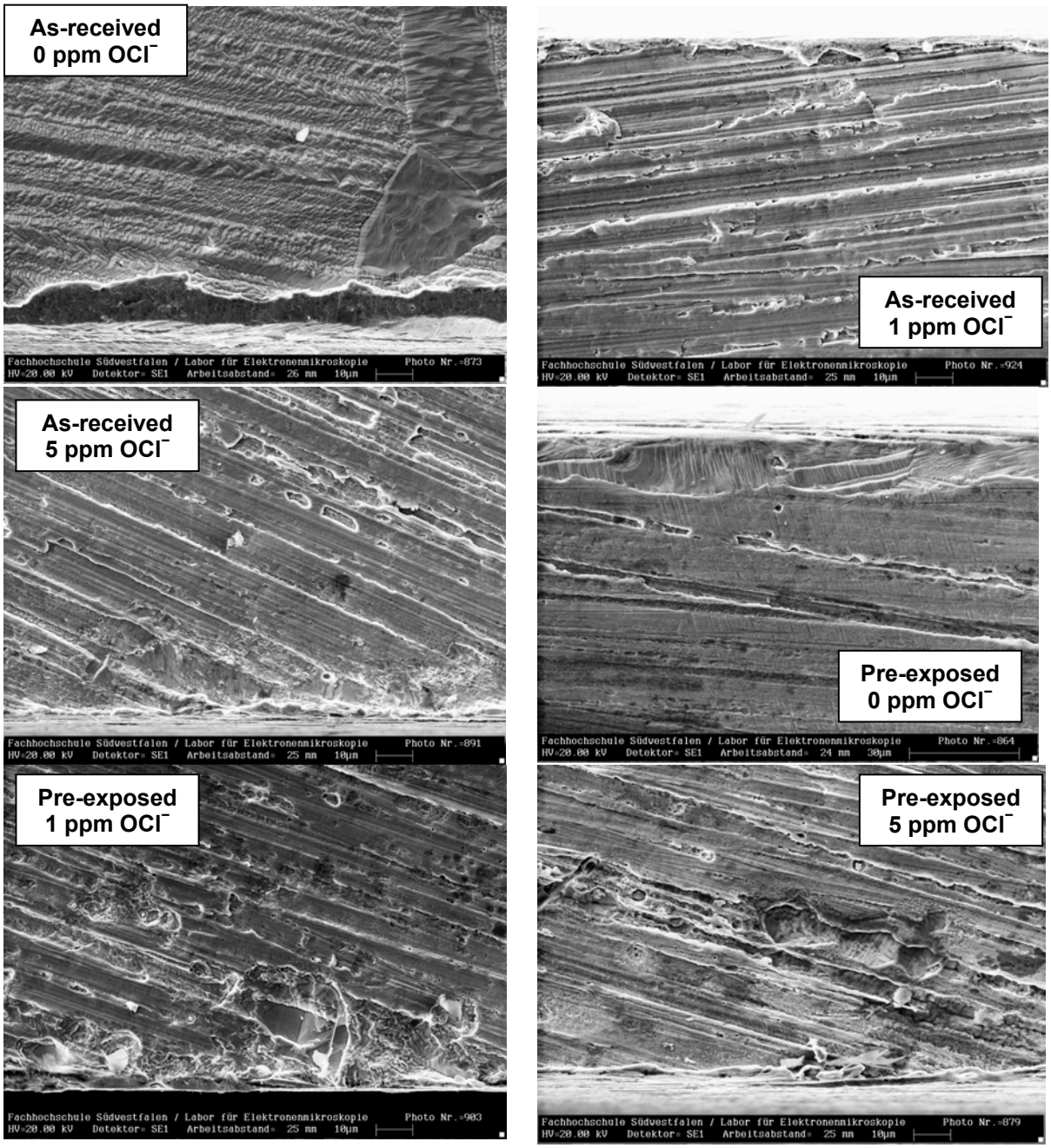

Figure 10: *CuNi90/10 coupons after 4 days rotation with 1500 rpm in artificial ASTM seawater at room temperature (etched surfaces). Effect of pre-exposure and presence of hypochlorite on the onset of flow induced localized corrosion (FILC).*

As exemplified by SEM investigations shown in Fig. 10, the flow induced localized material's attack was only slightly visible and occured only in the direct vicinity of the edges and had already stopped by 30 µm from the edges. It is evident that the local flow intensities at the sharp coupon edges are higher than some 200 µm away from the edges where the microelectrodes had been implemented into the coupon surface in the previous investigations [23, 24]. Therefore, it must be assumed that the effective local wall shear stresses which finally initiated the flow induced attack directly at the edges, are considerably higher than the local wall shear stress of 200 Pa calculated for the given geometries and the rotation speed of 1500 rpm.

Technically the equipment available did not allow higher rotation speeds to reach wall shear stresses great enough to initiate FILC on a wider range of coupon surface. Jet impingement experiments are under way to determine the critical wall shear stresses for different types of surface quality and hypochlorite concentration. It is already clear from the present evaluation of rotating cage experiments, that the critical wall shear stress of CuNi90/10 (UNS C70600) in artificial seawater is above 200 Pa, regardless of the presence of up to 5 ppm hypochlorite and prescaling of the surface. This result indicates that the previously reported critical wall shear stress of 43 Pa for UNS C70600 in artificial seawater [8] is effectively far too low.

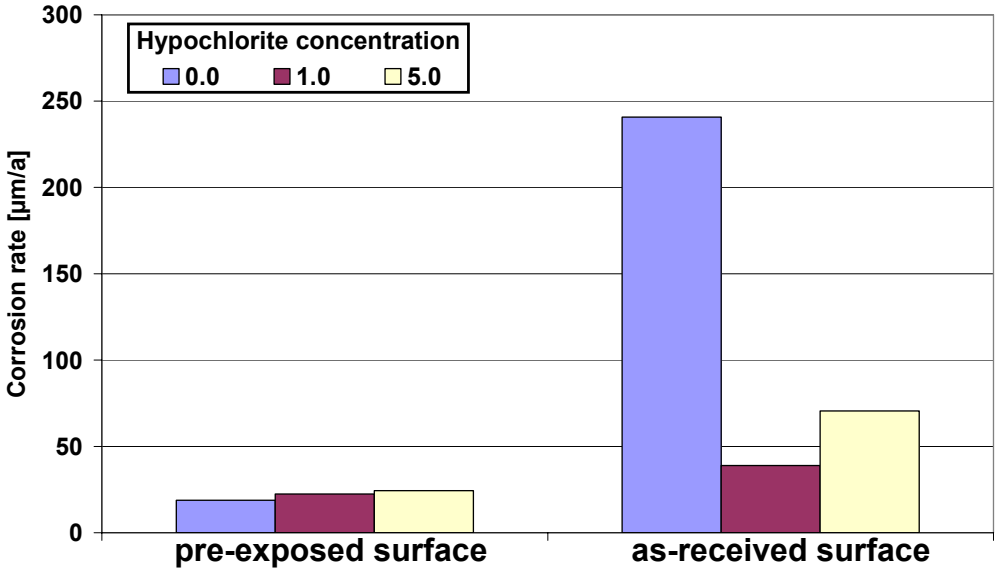

Figure 11: *Effect of pre-exposure and presence of hypochlorite on corrosion rate of CuNi90/10 coupons after 4 days rotation with 1500 rpm in artificial ASTM seawater at room temperature.*

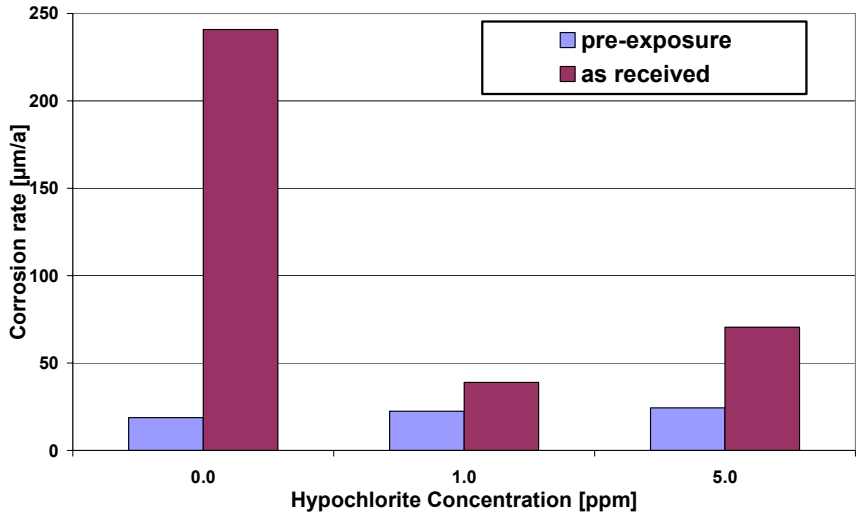

Figure 12: Effect of pre-exposure and presence of hypochlorite on corrosion rate of CuNi90/10 coupons after 4 days rotation with 1500 rpm in artificial ASTM seawater at room temperature.

Average values obtained from mass loss measurements on the rotated coupons from the 1500 rpm test series are summarized in Figs. 11-12. It is evident that scale formation during pre-exposure in artificial seawater is beneficial for reducing the general corrosion rate at high flow intensities. For pre-exposed material's surface the effect of hypochlorite on the general corrosion rate is not significant up to concentrations of 5 ppm. However, for the as-received surface the addition of small amounts of hypochlorite appears to be beneficial. Larger and generally not used hypochlorite concentrations (e.g. 5 ppm) seem to enhance the corrosion rate again.

4 Conclusions

The copper-nickel alloy UNS C70600 (CuNi90/10) exhibits excellent perfomance in artificial ASTM seawater at room temperature even at high flow intensities. Up to wall shear stresses of 200 Pa, only general corrosion and no flow induced localized corrosion was observed in high speed rotating cage experiments.

The flow resistance of CuNi90/10 is not significantly impaired by hypochlorite concentrations up to 5 ppm and is obviously significantly higher than expected from literature data which give 43 Pa as critical wall shear stress in seawater. The exact evaluation of the critical wall shear stresses with respect to hypochlorite effects and influences of pre-exposed filmed surface states will follow in a future investigation under jet impingement conditions.

Pre-exposure of the material in artificial seawater to allow formation of protective corrosion product layers is beneficial for the flow resistance and prevents enhanced corrosion by dissolved hypochlorite.

5 Acknoledgement

The co-authors (R.F., G.S., S.H. and K,S.) thank KME Germany AG for financial support and for the permission to publish this paper.

6 References

1. M.S. Parvizi et al, International Materials Reviews, **33** (1988)(4) 169
2. B.C Syrett et al., Corrosion, **35** (1979)(9) 409
3. L.E. Eiselstein et al., Corros. Sci., **23** (1983) (3) 223
4. W. W. Kirk and A.H. Tuthill, Copper-Nickel Condenser and Heat Exchanger Systems, Paper from a Seminar, The Application of Copper-Nickel Alloys in Marine Systems, Presented Jointly by ICA, CDA and Nickel Development Institute in Cooperation with Japan Copper Development Association, Korean Institute of Metals, Tokyo, Osaka and Nagasaki, Japan, Pusan and Kirje Island, Republic of South Korea, November, 1991
5. G. Schmitt, C. Bosch, M. Mueller, G. Siegmund, “A Probabilistic Model for Flow Induced Localized Corrosion“, CORROSION’2000, NACE International, Houston,TX, USA, 2000, Paper 049.
6. G. Schmitt, C. Werner, M. Bakalli, "Fluid Mechanical Interactions of Turbulent Flowing Liquids with the Wall - Revisited with a New Electrochemical Tool", CORROSION'2005, NACE International, Houston, TX, USA, 2005, Paper 05344.
7. G. Schmitt, M. Bakalli, “Quantification of Maximum Flow Intensities in Different Flow Systems for Assessing Boundary Conditions for Flow Induced Localized Corrosion”, Proc. EUROCORR’2007, 10-13 September 2007, Freiburg, Germany; DECHEMA, Frankfurt/Main, 2007.
8. K.D. Efird, Corrosion. **33** (1973) (1), 3-8.
9. J. Postlethwaite, S. Nesic, “Erosion-Corrosion in Single and Multiphase Flow”. In Uhlig's Corrosion Handbook, 2nd ed.; Edited by R. Winston Revie; John Wiley & Sons, Inc., 2000; Chapter 15, pp 249-272.
10. P. Roberge, “Erosion-Corrosion”. In “Corrosion Testing Made Easy”, B. C. Syrett Series Editor, NACE International, Houston, TX, USA, 2004.
11. British Standard: BSMA 18, Salt Water Piping Systems in Ships, August 1973,
12. L. Knutsson et al, Brit. Corros. J., 7 (1972) 20
13. M. Jasner and K. Steinkamp, “Why Copper Nickel 90/10 is the Optimum Pipe Material for Seawater Service”, Stainless Steel World 2002, Houston, USA
14. R. Francis, Materials Performance, **21** (1982)(8) 44
15. R. Francis, Corrosion, **26** (1985) (3) 205
16. W. Schleich, R. Feser, S. Siedlarek, „Electrochemical Behaviour of Copper-Nickel Alloy CuNi 90/10 in Chlorinated Seawater Under Stagnating Conditions”, CORROSION’2006, NACE International, Houston,TX,USA, 2006, Paper 07261
17. A Tuthill, “Guidelines for the Use of Copper Alloys in Seawater”, NiDI Publication 12003. 1988
18. G. Schmitt, W. Bruckhoff, K. Faessler, G. Bluemmel, “Flow Loop versus Rotating Probes – Correlations Between Experimental Results and Service Applications”, CORROSION’90, NACE International, Houston, TX, USA, 1990, Paper 23.
19. S. Papavinasam, R.W. Revie, M. Attard, A. Demoz, H. Sun, J.C. Donini, K. Michaelian, ”Inhibitor Selection for Internal Corrosion Control of Pipelines: 1. Laboratory Methodologies”, CORROSION’99, NACE International, Houston, TX, USA, Paper 1.
20. ASTM G184, “Standard Practice for Evaluating and Qualifying Oilfield and Refinery Corrosion Inhibitors using the Rotating Cage” (West Conshohocken, PA: ASTM, 2005).

21. F. Giralt, O. Trass, Canadian J. Chem. Eng. **53** (1975) 505-511.
22. F. Giralt, O. Trass, Canadian J. Chem. Eng. **54** (1976) 148-155.
23. G. Schmitt, K. Moeller, C. Werner, P. Plagemann, C. Deslouis, C. Bosch, M. J. Schöning, Y. T. Janabi, A. Belghazi, "Microturbulence Intensities in Disturbed Flow Regimes Quantified by Micro-electrochemical Measurements" Proc. 53th Ann. Meeting Intern. Soc. Electrochem. (ISE), "Electrochemistry in Molecular and Microscopy Dimensions", Düsseldorf, Germany, Sept. 15-20, 2002.
24. C. Deslouis, A. Belghazi, Y. T. Al-Janabi, P. Plagemann, G. Schmitt, "Quantifying Local Wall Shear Stresses in the Rotated Cage", CORROSION‘2004, NACE International, Houston, TX, USA, 2004, Paper 727.
25. E.S.Gonçalves, L. Poulsen, P. R. Ogilby, "Polymer degradation upon exposure to chlorinated water", EUROCOR'2006, 25-28-Sept.2006, Maastricht, The Netherlands, CD-ROM European Federation of Corrosion, The Institute of Materials, London, UK